

# Elucidation of caveolin 1 both as a tumor suppressor and metastasis promoter in light of epigenetic modulators

Moonmoon Deb · Dipta Sengupta · Swayamsiddha Kar ·  
Sandip Kumar Rath · Sabnam Parbin · Arunima Shilpi ·  
Subhendu Roy · Gautam Das · Samir Kumar Patra

Received: 27 June 2014 / Accepted: 13 August 2014 / Published online: 6 September 2014  
© International Society of Oncology and BioMarkers (ISOBM) 2014

**Abstract** Caveolin-1 (CAV1) is an integral part of plasma membrane protein playing a vital role in breast cancer initiation and progression. CAV1 acts both as a tumor suppressor as well as an oncogene, and its activity is thus highly dependent on cellular environment. Keeping this fact in mind, the recent work is designed to reveal the role of CAV1 in inhibiting cancer cell progression in presence of epigenetic modulators like 5-aza-2'-deoxycytidine (AZA), trichostatin A (TSA), S-adenosyl methionine (SAM) and sulforaphane (SFN). Forced expression of CAV1 by AZA, TSA, and SFN is correlated to induction of apoptosis and inhibition of cell migration in breast cancer. In breast cancer along with promoter DNA methylation, other epigenetic mechanisms are also involved in CAV1 expression. These observations clearly provide a new scenario regarding the role of CAV1 in cancer and as a possible therapeutic target in breast cancer.

**Keywords** Breast cancer · Caveolin-1 · DNA methylation · AZA · TSA · SFN · SAM

---

M. Deb · D. Sengupta · S. Kar · S. K. Rath · S. Parbin · A. Shilpi ·  
S. K. Patra (✉)  
Epigenetics and Cancer Research Laboratory, Biochemistry and  
Molecular Biology Group, Department of Life Science, National  
Institute of Technology, Rourkela, Odisha 769008, India  
e-mail: samirp@nitrkl.ac.in

S. K. Patra  
e-mail: skpatra\_99@yahoo.com

S. Roy  
Drs. Tribedi & Roy Diagnostic Laboratory, 93, Park Street,  
Kolkata 700016, India

G. Das  
Department of Surgery, Calcutta National Medical College,  
Kolkata 700014, India

## Introduction

Caveolin-1 (CAV1) protein has been identified as a marker indispensable for membrane caveolae formation, maintenance, and function. Caveolae is responsible for various cellular processes in normal and pathophysiological states, including cancer progression and hormone refractory diseases [1–7].

In animal model, studies targeted disruption of CAV1 and homologous recombination created CAV1-null mice have shown that natural presence of caveolae is absent from various cell types resulting in severe physical limitations in CAV1-disrupted mice. Some of those include impaired nitric oxide and calcium signaling in cardiovascular system, causing aberrations in endothelium-dependent relaxation, contractility, and maintenance of myogenic tone. In addition, CAV1 knockout mice lung displayed thickening of alveolar septa caused by uncontrolled endothelial cell proliferation and fibrosis [8, 9]. Endothelial CAV1 and caveolae are necessary for both rapid and long-term mechanotransduction in intact blood vessels [6, 10–12]. Lack of caveolae formation is associated with degradation and redistribution of CAV2, defects in the endocytosis of albumin (a caveolar ligand and a major plasma protein that transports and scavenges metabolites and endotoxic substances, respectively), and a hyperproliferative phenotype in tissues and cultured embryonic fibroblasts from the CAV1 null mice [9]. Schubert et al. [13] has recently examined the role of “non-muscle” caveolins (CAV1 and CAV2) in skeletal muscle biology and found that skeletal muscle fibers from male CAV1(−/−) and CAV2(−/−) mice show striking abnormalities, such as tubular aggregates, mitochondrial proliferation/aggregation, and increased numbers of M-cadherin-positive satellite cells, which became more pronounced with ageing. CAV1 knockout (KO) mice were observed to be completely devoid of caveolae. Lewis lung carcinoma cells implanted into CAV1 KO mice had increased tumor microvascular permeability, angiogenesis, and growth [6].

Cell culture and biochemical findings evidenced that CAV1 is a tumor suppressor gene and a negative regulator of the V-Src avian sarcoma (Schmidt-Ruppin A-2) viral oncogene homolog (v-Src), H-Ras, protein kinase A, protein kinase C (PKC) isoforms, and Ras-p42/44 mitogen-activated protein (MAP) kinase cascade within caveolae [1]. Loss of heterozygosity analysis implicates chromosome 7q31.1 (where CAV1 gene is localized to a suspected tumor suppressor locus D7S522), in the pathogenesis of multiple types of human cancer, including breast, ovarian, prostate, and colorectal carcinoma, as well as uterine sarcomas and leiomyomas. For example, CAV1 expression in mammary adenocarcinoma (MTLn3) cells inhibits epidermal growth factor (EGF)-stimulated lamellipod extension and cell migration, blocks their anchorage-independent growth, and thus induces a non-motile phenotype by blocking the EGF-induced activation of the p42/44 MAP kinase cascade [14].

On the other hand, CAV1 can also function as tumor metastasis-promoting molecule which is not likely to its cell growth inhibitory function. For example, higher expression of CAV1 induces filopodia formation in lung adenocarcinoma with enhanced metastasis [14]. Puzzling question arises, why a tumor suppressor gene whose inactivation is necessary for cell transformation and tumor induction can be re-expressed to facilitate tumor progression? Such a paradox is not restricted only to CAV1. It is apparent that other molecules, including E-cadherin, CD44, granulocyte/macrophage colony-stimulating factor (GM-CSF), RAR- $\beta$ 2, and  $\alpha$ - and  $\beta$ -catenin, have also been reported to impart the virtual opposite function in tumorigenesis. The promoters of the various cell surface adhesion marker genes, including CAV1, are inactivated in association with promoter CpG hypermethylation at the onset of tumor development and remains thereafter methylated in full-blown tumors but were found to be re-expressed in metastatic foci and lymph nodes. Since these genes are mostly inactivated by DNA methylation, their reactivations certainly need demethylation activity [1, 15]. For instance, messenger RNA (mRNA) and protein expression of CAV1 are frequently lost in multiple cancers. At the cancer onset, CAV1 gene is repressed by DNA methylation, while re-expression occurs just before metastasis (reviewed in Patra [1]).

Herein, we have sought to explain the mysterious behavior of CAV1 in breast cancer. Strained expression of CAV1 by 5-aza-2'-deoxycytidine (AZA, a well-established DNA (cytosine-5)-methyltransferase inhibitor) [16], trichostatin A (TSA, an effective histone deacetylase inhibitor) [17, 18], and sulforaphane (SFN, a newly developed histone deacetylase (HDAC) inhibitor) [19] has a significant role in breast cancer inhibition. On the other side, S-adenosyl methionine (SAM, the universal methyl donor) [20] does not show any major effect in breast cancer inhibition. We also explain that DNA methylation has an important role in CAV1 expression in breast cancer tissue sample and cell lines. However, promoter

DNA methylation is not the sole regulatory mechanism for CAV1 expression in breast cancer. Along with DNA methylation, perhaps histone acetylation also plays important in CAV1 expression in breast cancer cell lines.

## Materials and methods

### Tissue samples and immunohistochemistry

Ninety-five formalin-fixed paraffin embedded (PEFF) breast cancer tissue samples were collected from Drs. Tribedi & Roy Diagnostic Laboratory (Kolkata, India). Formalin-fixed paraffin embedded specimens were slice into 0.5  $\mu$ m and subjected to antigen retrieval with Tris-EDTA buffer, endogenous peroxidase blocking, and rinsed with Tris-buffered saline (TBS) containing 0.025 % Triton X-100 (TBS-T). Rabbit polyclonal anti-CAV1 (Santa Cruz), rabbit polyclonal anti-DNA methyltransferase (DNMT) 1 (Santa Cruz), rabbit polyclonal anti-DNMT3A (Santa Cruz), and rabbit polyclonal anti-DNMT3B (Santa Cruz) were used as primary antibodies. The secondary antibody was used anti-rabbit (Invitrogen). After incubation with anti-CAV1 antibody at 4 °C overnight, the specimens were rinsed with TBS and incubated at room temperature for 1 h with secondary antibody. After rinsing with TBS, all specimens were color-developed with 3,3'-diaminobenzidine (DAB) Liquid Substrate System tetrahydrochloride (Sigma).

### Cell culture

MCF7 and MDA-MB-231 were purchased from the National Centre for Cell Sciences, Pune (NCCS), and both cell lines were derived from metastatic site. MCF7 and MDA-MB-231 were cultured in Dulbecco's-modified Eagle's and Minimum Essential Medium Eagle's, respectively, which were medium supplemented with 10 % fetal calf serum and penicillin (100 unit/ml)–streptomycin (0.1 mg/ml). Stock solutions of 5-aza-CdR (Sigma) TSA (Sigma) and SFN (Sigma) were dissolved in dimethylsulfoxide (DMSO). Immediately before use, stock solutions were further diluted in medium.

Cells were trypsinized and cell numbers counted by a hemocytometer, and the living cells were calculated by Trypan blue staining (0.2 % v/v). Cells ( $5 \times 10^5$ ) were seeded into each 60-mm dish followed by treatment next day.

### Cell viability assay

Breast cancer cell lines were counted by a hemocytometer. Viability was determined by Trypan blue staining. For each cell line,  $5 \times 10^3$  cells were seeded in each well of 96-well microtiter plates. After 24-h incubation, growth medium was replaced with experimental medium containing epigenetic

modulator at different concentrations. For determining the concentrations of AZA, SAM, TSA, and SFN that inhibited cell proliferation by 50 % (IC<sub>50</sub>), the cells were treated with at final concentrations of AZA (0.5, 5, 10, 15, and 20  $\mu$ M) for 72 h and TSA (25, 50, 100, 250, and 500 nM), SFN (1, 5, 7.5, 10, and 20  $\mu$ M), and SAM (5, 10, 25, and 50  $\mu$ M) for 24 h. Growth medium containing DMSO as a control for AZA, TSA, and SFN whereas without DMSO control for SAM. Cell proliferation was determined by [3-(4,5-dimethylthiazol-2-yl)-2,5-diphenyltetrazolium bromide (MTT) assay. MTT (0.8 mg/ml) solution was prepared from stock MTT solution (5 mg/ml PBS, pH 7.2). One hundred-microliter MTT solution was added to each well and incubated at 37 °C allowing for 4 h. The supernatant was removed and 100  $\mu$ l of DMSO was added into each well. The absorbance was measured at 570 nm, and the results expressed as the mean of three replicates as a percentage of control (taken as 100 %).

#### RNA extraction and qRT-PCR

Two cell lines were treated with AZA for 72 h and TSA, SFN, and SAM for 24 h. After treatment, total RNA was extracted with Tri Reagent (Sigma) according to the manufacturer's instructions. Quantitative reverse transcription (qRT)–PCR was performed using 1  $\mu$ g of total RNA RevertAid First Strand cDNA Synthesis Kit (Thermo Scientific) and SYBR® Green JumpStart™ Taq ReadyMix in the Realplex4 Eppendorf system. The mRNA level was normalized to  $\beta$ -actin (Elongation Factor 1-  $\alpha$ ), as we have described [21]. The primer sequences for CAV1 amplification were 5'-ACCCAC TCTTGAGCTGTTG-3' and 5'-GAACTTGAAATTGG CACCAGG-3' (producing a fragment of 139 bp).  $\beta$ -Actin was used as an internal control, and primer sequences were 5'-CTGGAACGGTGAAGGTGACA-3' and 5'-AAGGGA CTTCTGTAAACAAACGCA-3' (producing a fragment of 141 bp).

#### Methylation-specific PCR

Genomic DNA was isolated from each treated cells by phenol chloroform method. Two microgram of genomic DNA was bisulfite converted by EpiTect Bisulfite Kit (Qiagen) according to the manufacturer's instructions. Bisulfite-treated DNA was then used as template in PCR reactions for PCR analysis. For identifying the methylation on the CAV1 CGI using methyl-specific PCR (MSP), 5'-TTATTTTGTTGAGATGA TGTATTGC-3' (sense) and 5'-GAACAAAAAACGAATA AAAACGTT-3' (antisense) were used for methylated form (producing a fragment of 151 bp with annealing at 60 °C), and 5'-TTTTGTTGAGATGATGTATTGTGA-3' (sense) and 5'-CAAACAAAAACAAATAAAAACATT-3' (antisense)

were used for unmethylated form (producing a fragment of 152 bp with annealing at 60 °C).

#### Immunocytochemistry

Breast cancer cell lines were grown on glass coverslips. In brief, subconfluent cells were fixed by ice-cold methanol and were permeabilized by 0.25 % Triton X-100 in PBS. Cells were incubated with 1 % BSA in PBST for 30 min to block unspecific binding of the antibodies. The endogenous peroxidase activity was blocked by incubation in 5 % H<sub>2</sub>O<sub>2</sub> in methanol for 20 min. Rabbit polyclonal anti-CAV1 (Santa Cruz) was incubated overnight at 4 °C. The cells were washed in PBS then incubated with HRP-conjugated anti-goat secondary antibody (Santa Cruz Biotech) for 1 h followed by another wash. Finally, reactions were visualized by incubation with DAB (substrate and chromogen) and counterstaining with Mayer's hematoxylin. For negative control, the cells were incubated overnight with dilution buffer (no primary antibody) [22].

#### Western blot analysis

Cells were grown to 80–85 % confluence and harvested, and cellular proteins were extracted with lysis buffer (RIPA buffer, Sigma) containing cocktail of protease inhibitors (Sigma). Total protein was separated on a SDS-polyacrylamide gel and electroblotted to PVDF membranes (Millipore). Protein containing membranes was block with 5 % skim milk in 0.1 % Tween 20 in TBS. Then, the membranes were incubated at 4 °C overnight with rabbit polyclonal anti-caveolin (Santa Cruz) and mouse monoclonal  $\beta$ -actin (Santa Cruz) (Sigma) antibodies. The membranes then were developed with peroxidase-labeled secondary antibodies, anti-rabbit (Invitrogen), and anti-mouse (sigma) by SuperSignal West Femto Chemiluminescent Substrate (Thermo Scientific).  $\beta$ -Actin protein levels were used as a control for adequacy of equal protein loading.

#### Chromatin condensation assay

After treatments with epigenetic modulators, cells were stained with Hoechst 33342 stain (1 mg/ml, Invitrogen) and incubated for 10 min at 37 °C, and images were taken under epifluorescent microscope (Olympus IX71). Condensed nucleus was counted against total number of nucleus in the field, and the percentage of apoptotic nuclei were calculated and plotted graphically [23].

### Analysis of cell migration by wound healing assay

In wound healing assay, the cells grew up to 90 % confluence, and a scratch was made on a uniform layer of the cells using a sterile micropipette tip, and the cells were washed with PBS to remove debris. Photographs of the same area of the wound were taken after 24-h treatment with AZA, SAM, TSA, and SFN to measure the width of the wound.

### Preparation and transfection of synthetic siRNA

The small-interfering RNAs (siRNA) against CAV1 (CAV1-I siRNA) were 5'-AGACGAGCUGAGCGAGAAC-3' (sense) and 5'-CUUCUCUGCUCAGCUCGUCUGC-3' (antisense) and (CAV1-II siRNA) 5'-CAUCUACAAGCC CAACAACTT-3' (sense) and 5'-GUUGUUGGGCUUGU AGAUGTT-3' (antisense) [24–26]. These siRNAs were perfectly matched with CAV1 mRNA sequence which was evaluated by NCBI blast. CAV1 and control siRNA (Santa Cruz) were transfected into the cells with use of Lipofectamine 2000 transfection reagent (Invitrogen) according to the manufacturer's instructions.

### Statistical analysis

All data are presented as means $\pm$ SD. Statistical analysis was performed using the Student's *t* test by SPSS software. Values of  $p<0.05$  were considered as significant value.

### Ethical approvals

This study was deemed exempt from ethics approval from National Institute of Technology, Rourkela, and work supporting approval from collaborating pathological laboratories, and consent was not required due to use of cell lines.

## Results

### CAV1 and DNMT expression in breast cancer tissue samples

The role of CAV1 as tumor promoter versus tumor suppressor is heavily dependent upon the tumor stage. CAV1 expression was assessed by both immunohistochemistry and RT-PCR techniques in 95 formalin-fixed paraffin embedded (FFPE) tissue samples and 25 post-operated breast cancer samples, respectively. Among FFPE breast cancer tissue samples, 55 were metastasis stage tissues and 40 were primary stage tissues. Among 25 post-operated tissue samples, 15 were metastasis stage tissues and 10 were primary stage tissues (Fig. 1 and Table 1).

At RNA level expression, 12 samples among the 15 post-operated metastasis stage tissues (80 %) exhibited CAV1 upregulation whereas among 10 post-operated primary stage tissues, 9 (90 %) samples showed CAV1 downregulation with respect to normal breast epithelial cell. During protein level expression analysis, high level of CAV1 protein expression was observed in 40 metastasis stage FFPE tissue samples (72.73 %), whereas 32 post-operated FFPE tissue samples

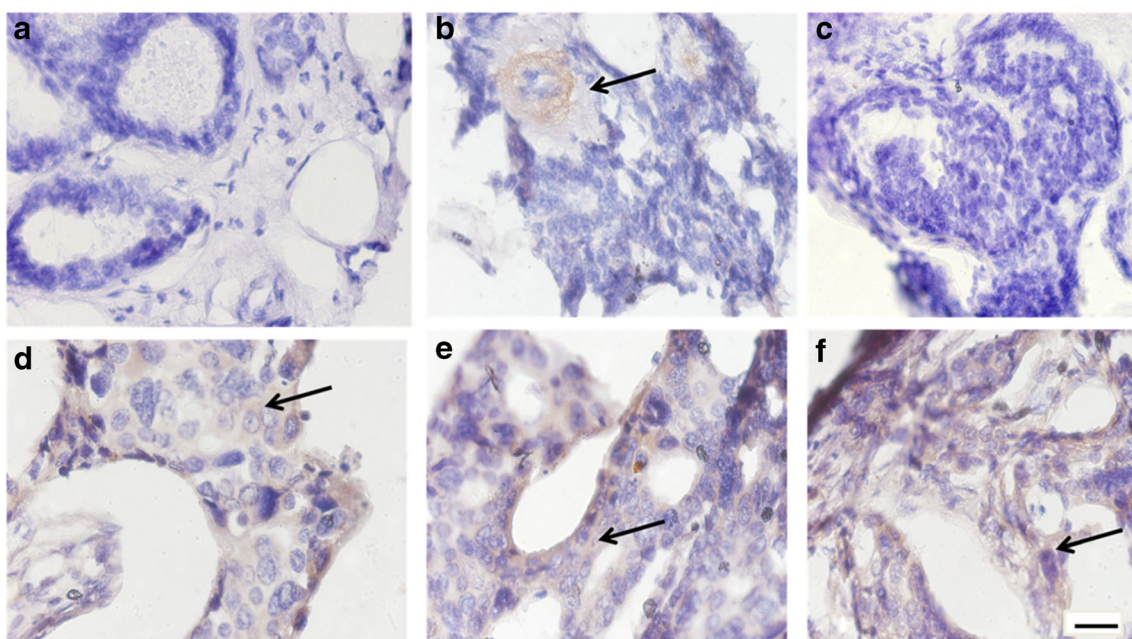


**Fig. 1** Immunohistochemical analysis of the CAV1: **a, b, c** Primary stage FFPE tissue sample shows nearly negative or very low (arrow) protein expression whereas **d, e, f** are metastasis stage FFPE tissues showing high levels of protein expression (arrow). Scale bar=40  $\mu$ m

**Table 1** CAV1 expression in FFPE and post-operated breast cancer tissue samples

Clinical breast cancer sample	Number of samples	Age	Stage of cancer/number of sample	CAV1 expression in RNA/protein level (%)	Absence of CAV1 expression in RNA/protein level (%)
Post-operated tissue sample (analyzed for RNA level CAV1 expression)	25	$\leq 65$	Metastasis stage/15	80 (12 samples)	20 (3 samples)
			Primary stage/10	10 (1 samples)	90 (9 samples)
FFPE tissue sample (analyzed for protein level CAV1 expression)	95	$\leq 50$	Metastasis stage/25	88 (22 samples)	12 (3 samples)
			Primary stage/75	20 (15 samples)	80 (60 samples)

(80 %) showed low or negative CAV1 expression (Fig. 2 and Table 1).

Previous studies have reported that CAV1 expression in cancer is regulated by promoter methylation in breast [27], colorectal [28], and prostate cancers [29]. It has also been reported that CAV1 expression is upregulated in ovarian cancer [30], non-small cell lung cancer [26], and prostate cancer [31] after treatment with DNMT inhibitor, 5-aza-CdR. DNMT expression plays an important role in CAV1 expression in different stages of cancer. In reference to this data, the expression of DNMT1, DNMT3A, and DNMT3B in FFPE tissue samples was analyzed. DNMT1 and DNMT3A were expressed in all types of tissue samples whereas DNMT3B expression was comparatively lower with respect to the other two DNMTs (Fig. 3). DNMT1 and DNMT3A expression did not display significant difference in metastasis and primary tissue samples; however, CAV1 expression was differentially varied in two different stages.

### Effect of epigenetic modulators on cell viability

To confirm whether CAV1 expression was controlled by epigenetic modifications, we treated two breast cancer cell lines of different stages with four epigenetic modulators, each with its own distinct effect on cell viability at different concentrations. AZA [32, 33], TSA [34, 35], and SFN [19] have been reported to be potent drugs against breast cancer. Cell viability was observed to decrease with increase in AZA, TSA, and SFN concentrations (Fig. 4). But an exception was observed in case of SAM-treated cells. Cell viability did not decrease significantly and remains approximately similar to the viability of control (untreated) cells after 24-h treatment (Fig. 4). Changes in cell viability indicate that variations made by epigenetic modulators drive the cells towards the changing viability level. In case of MCF7, 50 % cell viability was observed at a concentration of 17  $\mu$ M for AZA, 75 nM for TSA, and 6  $\mu$ M for SFN-treated cells. In case of MDA-MB-231, 50 % cell viability was observed at a concentration of 19  $\mu$ M for AZA, 100 nM for TSA, and 8  $\mu$ M for SFN-treated cells (Fig. 4). Twenty-micromolar concentration of SAM was used for the treatment for both cell lines. Future experiments proceeded with these particular concentrations.

Previous reports had emphasized that CAV1 involved in cell growth regulation [27, 36]. From the above observations, it could implicate that epigenetic modulators may affect and modify the epigenetic modifications of CAV1 and lead to changes in CAV1 expression which can be correlated to cell growth. Further experiments were performed to confirm the above findings.

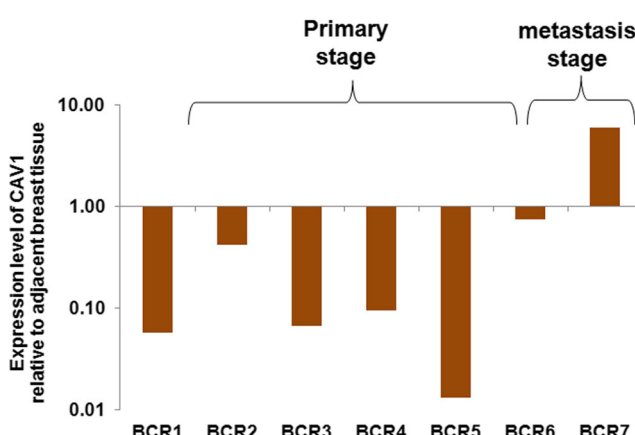


**Fig. 2** CAV1 mRNA levels in seven post-operated breast cancer tissue samples were measured by reverse transcription–PCR. Four samples (BCR1, BCR2, BCR3, BCR4, and BCR5) were primary stage tissue samples, and BCR6 and BCR7 were metastasis stage breast cancer samples. CAV1 was downregulated in BCR1, BCR2, BCR3, BCR4, BCR5, and BCR6 and upregulated in BCR7 with log-scale analysis. The CAV1 mRNA level in adjacent tissues was normalized to 1

### Role of DNMT inhibitor, AZA, in regulating CAV1 mRNA level

The DNMT inhibitor, AZA, decreases the methylation level by inhibiting the DNMT enzyme. MCF7 and MDA-MB-231 are described as non-aggressive and aggressive cell lines, respectively. Previous reports have claimed that higher CAV1 mRNA expression is

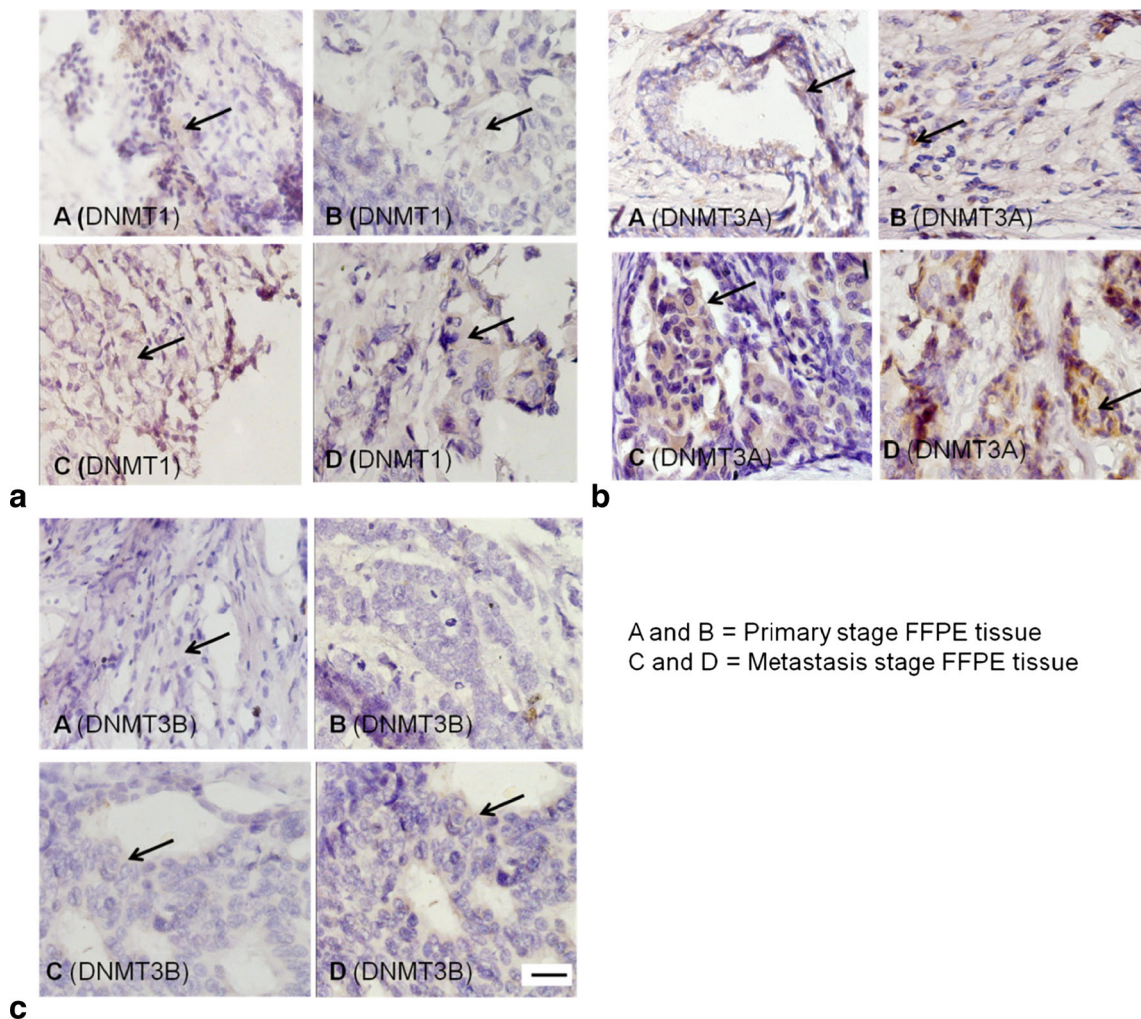


**Fig. 3** Immunohistochemical analysis of the DNMT1, DNMT3A, and DNMT3B expressions: **a** DNMT1 A and B are primary, and C and D are metastasis stage FFPE tissues showing (arrow) protein expression. **b** DNMT3A A and B are primary, and C and D are metastasis stage FFPE

tissues showing (arrow) protein expression. **b** DNMT3B A and B are primary, and C and D are metastasis stage FFPE tissues showing (arrow) protein expression. Scale bar=40  $\mu$ m

seen in case of MBA-MB-231 in comparison to MCF7 cells [37]. After AZA treatment, CAV1 mRNA expression increased in both cell lines. CAV1 mRNA level showed 1.96-fold ( $p<0.05$ ) and 3.13-fold ( $p<0.05$ ) (Fig. 5) increase in MCF7- and MDA-MB-231 AZA-treated cells, respectively.

#### Effect of HDACs—TSA and SFN—on the expression level of CAV1 mRNA

CAV1 expression has been known to be affected by TSA treatment in different types of cancer such as ovarian cancer [30] and breast cancer [38]. However, the effect of SFN treatment on breast cancer cells has not yet been reported. It is seen that CAV1 expression increased by TSA and SFN treatments. Fold of increase in CAV1 mRNA level was 35.25 in case of MCF7 and 42.4 in MDA-MB-231 cells after TSA treatment

whereas SFN treatment resulted in an increase of 11-fold in CAV1 expression in MCF7 and 23.3-fold in MDA-MB-231 ( $p<0.05$ ) (Fig. 5). Henceforth, it can be said that induction of CAV1 expression by TSA and SFN is associated with cancer inhibition.

#### Universal methyl group donor, SAM, changes CAV1 mRNA level

SAM has also been described earlier to be involved in breast cancer prevention [39, 40]. For the first time, we have reported that SAM treatment changes CAV1 expression in breast cancer cell lines. SAM treatment decreased CAV1 expression by 1.29-fold in MCF7 and increased by 1.57-fold in MDA-MB-231 ( $p<0.05$ ) (Fig. 5). Thus, after SAM treatment, CAV1 expression increases in MDA-MB-231 and decreases in MCF7 cell lines.

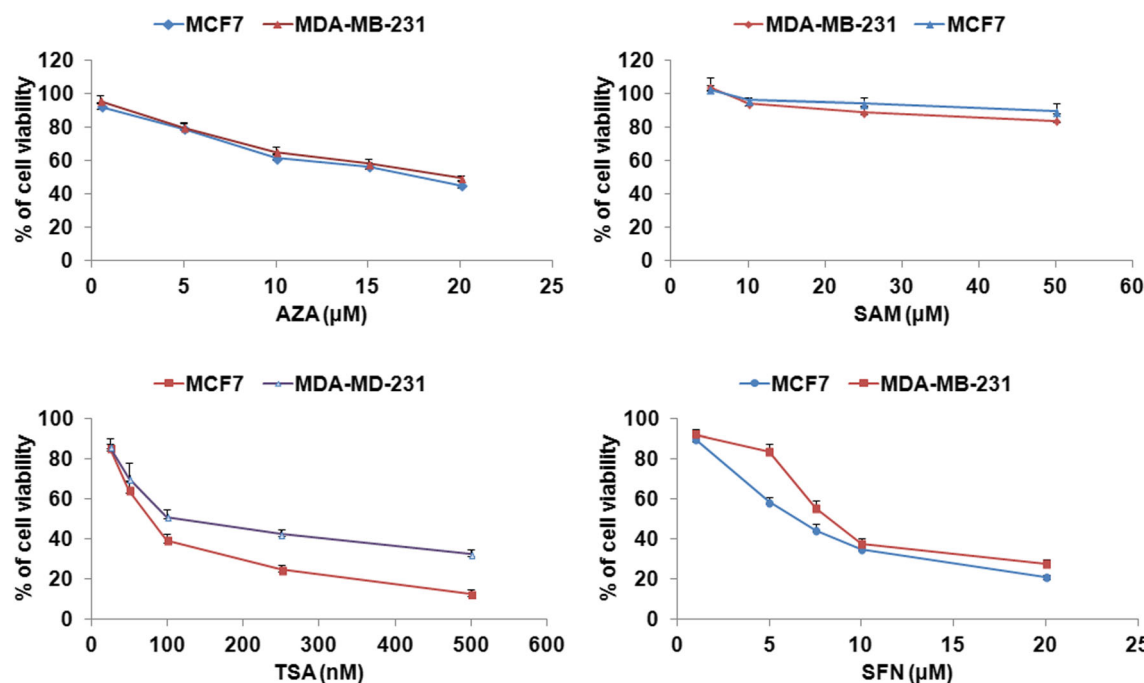


**Fig. 4** Cell viability assay of MDA-MB-231 and MCF7. Percentage of proliferation was calculated by  $(\text{Abs}_{\text{treated cells}} - \text{Abs}_{\text{background}})/(\text{Abs}_{\text{control cells}} - \text{Abs}_{\text{background}}) \times 100$  ( $n=3$ , mean $\pm$ S.D.)  $P<0.05$

#### Role of CpG island methylation in regulating CAV1 gene expression

CAV1 was upregulated after treatment with epigenetic modulators. It can thus be assumed that different epigenetic modifications directly or indirectly control CAV1 expression in breast cancer cell lines. Henceforth, methyl-specific PCR (MSP) was performed to analyze the established methylation pattern in CAV1 promoter region. Promoter region was retrieved by <http://www.genomatix.de/> software and analyzed by UCSC genome browser (Fig. 6a). Meth primers and

bisulfite primers were designed by MethPrimer design tool (<http://www.urogene.org/methprimer/>). Upstream region of CAV1 gene (Chr7: 116,164,718–116,164,869 and 151 bp) was amplified by meth primers. A total of three CpG site methylations (Fig. 6b) were analyzed by meth primers. Seven post-operated breast cancer tissues were examined by MSP. These results indicate that unmethylated promoter regions were predominant in breast cancer tissue samples. However, partial methylation was observed in four primary post-operated breast cancer tissues—BCR1, BCR2, BCR3, and BCR4. Whereas, promoter regions of two metastasis tissue samples—BCR6 and BCR7—were totally unmethylated (Fig. 6c(A)). After treatment with AZA, SAM, TSA, and SFN, notable changes were observed in CAV1 promoter methylation. AZA-treated cells showed unmethylated CAV1 promoter whereas CAV1 promoter region was methylated in TSA- and SFN-treated cells. Cells treated with SAM and untreated control cells predominantly exhibited unmethylated and partially methylated promoters in MCF7 (Fig. 6c(B)) and MDA-MB-231 (Fig. 6c(C)).

Epigenetic modulators induced CAV1 upregulation mediated cancer cell growth inhibition

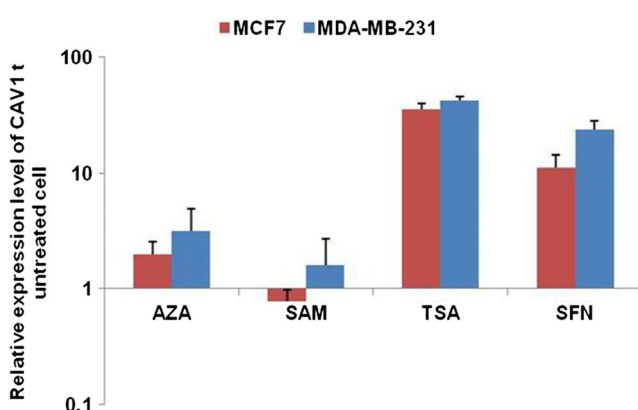


**Fig. 5** CAV1 mRNA level was increased on the onset of AZA, SAM, TSA, and SFN treatments in both MCF7 and MDA-MB-231. CAV1 mRNA level was measured by reverse transcription–PCR. The CAV1 level in DMSO-treated cells for AZA, TSA, and SFN and without DMSO-treated cells for SAM was normalized to 1 ( $n=3$ , mean $\pm$ S.D.)  $P<0.05$

Immunocytochemistry and Western blot analyses reveal that CAV1 expression increases at the protein level after treatment with epigenetic modulators in both cell lines (Figs. 7 and 8). However, CAV1 expression was higher in the case of TSA- and SFN-treated cells than in the AZA- and SAM-treated cells

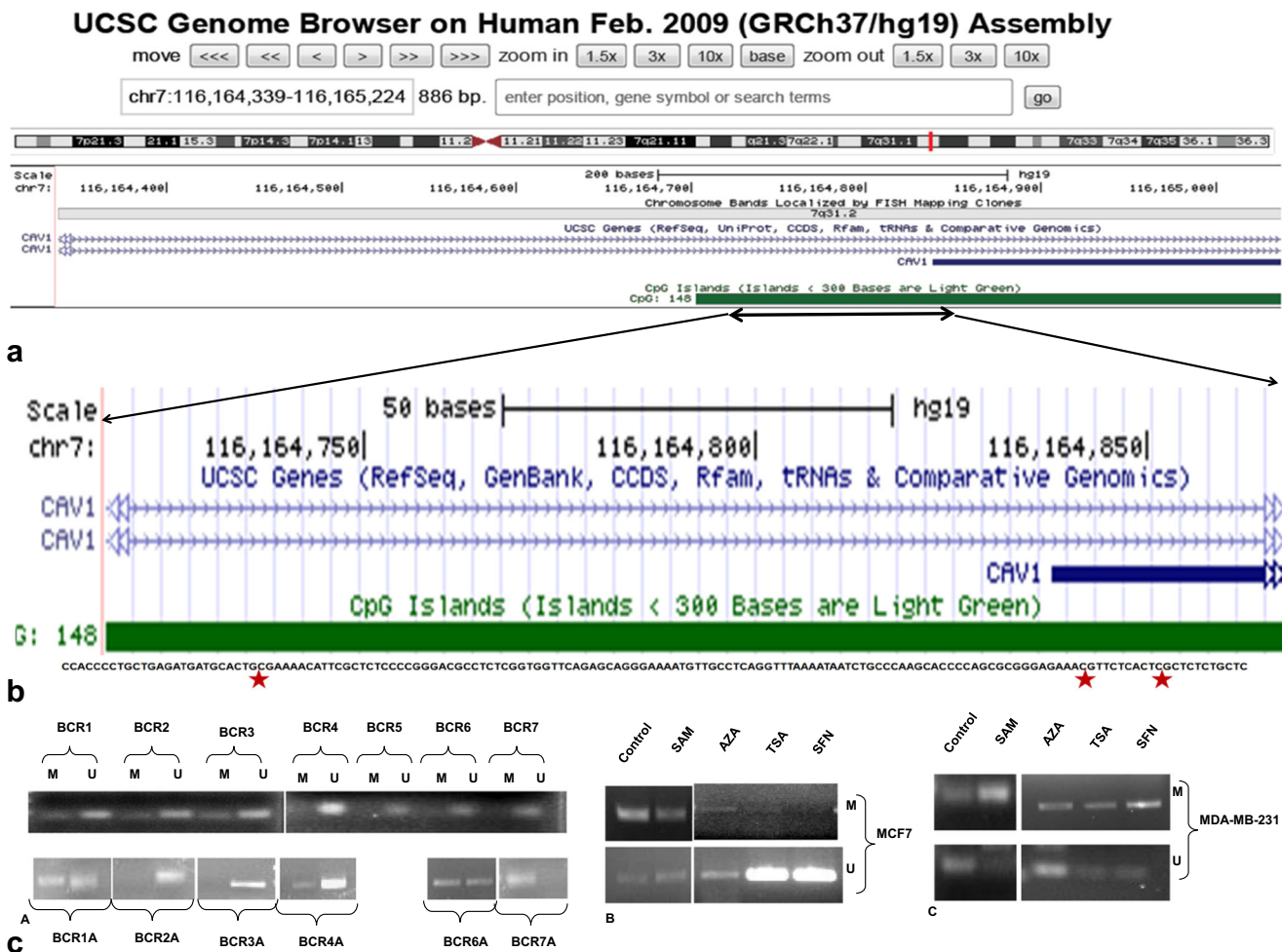


**Fig. 6** Methylation detection using methylation-specific PCR. **a** University of California Santa Cruz (UCSC) genome browser view of CAV1 promoter region and **b** distribution of CpG island. **c** The primer pairs point toward the region that was analyzed by methylation-specific PCR in

post-operated breast cancer tissue samples and adjacent tissue (A), MCF7 (B), and MDA-MB-231 (C). Three CpG sites (red stars) are covered by primers. *U* results with primers specific for unmethylated sequence, *M* results with primers specific for methylated sequence

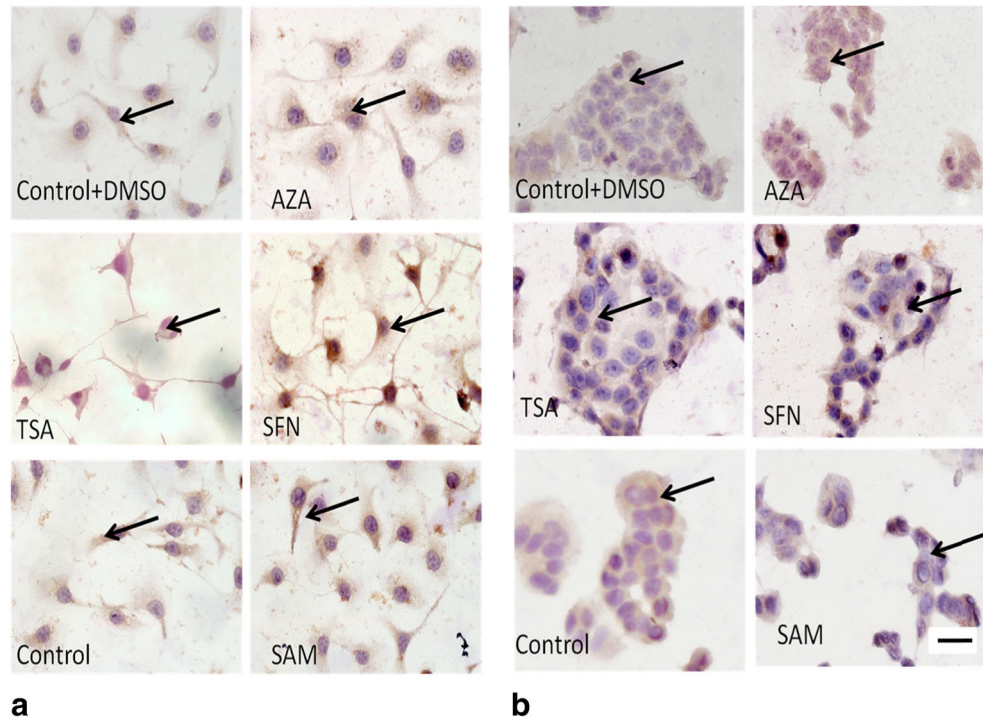
in both cell lines. Cells that were subjected to AZA, TSA, and SFN treatments show significant cancer growth inhibition than SAM treatment.

During apoptosis, chromatin becomes inert, highly condensed, then fragmented, and packaged into apoptotic bodies [41]. Highly stained nuclei by Hoechst 33342 can be comparable to apoptotic cells. In AZA, SAM-, TSA-, and SFN-treated cells, the percentage of condensed nuclei were 26.66, 9.33, 65.66, and 66.78 % in the case of MCF7 (Fig. 9a, c) and 7.68, 2.45, 39.66, and 41.78 % in the case of MDA-MB-231 (Fig. 9b, c), respectively, whereas control and DMSO-treated control cells were shown to be 7.21 and 6.63 % in MCF7 (Fig. 9a, c) and 2.11 and 2.77 % in MDA-MB-231, respectively (Fig. 9a, c). The result indicates that nuclei of MCF7 and MDA-MB-231 cells which were treated with AZA, TSA, and SFN exhibit condensed and bright nucleus while the untreated cells exhibit very less amount of condensed chromatin. Unlike the other three

modulators, SAM-treated cells exhibit different results. The percentage of condensed nuclei after SAM treatment are very low, i.e., 9.33 % in MCF7 and 2.16 % in MDA-MB-231, which are approximately same as that of the control (Fig. 9a–c).

Wound healing assay was performed for analyzing the cell migration after treatment with various epigenetic modulators [42]. We performed in vitro wound healing assay to assess the role of AZA, SAM, TSA, and SFN in cell migration. The results showed that the migration of AZA-, TSA-, and SFN-treated cells appeared significantly slower compared to control and SAM-treated cells in both cell lines. Among them, TSA and SFN were most effective in inhibiting cell migration in MCF7 and MDA-MB-231 (Fig. 10). Nuclear condensation and wound healing assays clearly indicate that treatment with modulators induces cell death and reduction in aggressiveness of MCF7 and MDA-MB-231 cells by different proportions.

**Fig. 7** Immunocytochemistry analysis of CAV1 showed that epigenetic modulators trigger CAV1 expression (arrow) in **a** MCF7 and **b** MDA-MB-231 cells with respect to specific untreated control cells. Scale bar=40  $\mu$ m

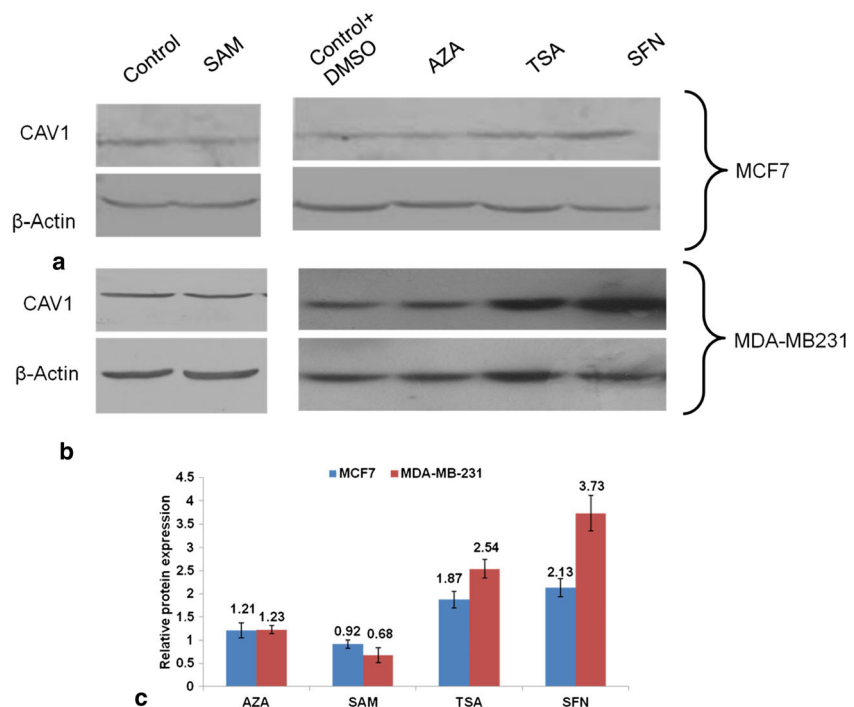
**a****b**

CAV1 knockdown cells behaved like epigenetic modulator untreated cell lines

Above results clearly explain that epigenetic modulators increase CAV1 expression and inhibit cancer progression. We hypothesized that AZA-, TSA-, and SFN-mediated CAV1 overexpressions are correlated to breast cancer inhibition. In

order to prove this hypothesis, we treated both the cell lines with CAV1 siRNA (Fig. 11a). CAV1 knockdown cells behaved like untreated cells. Moreover, percentage of condensed chromatin partially decreased after CAV1 knockdown (Fig. 11b(A), (B)). Cell migration was near about the same with control siRNA-treated cells cell in MCF7 and MDA-MB-231 (Fig. 11c(A), (B)).

**Fig. 8** MCF7 (**a**) and MDA-MB-231 (**b**) cell lysates were subjected to Western blotting with antibody specific for CAV1 after treatment with epigenetic modulators. Anti- $\beta$ -actin was used to confirm equal loading. **c** The graphical representation of relative expression level of CAV1 protein after treatment



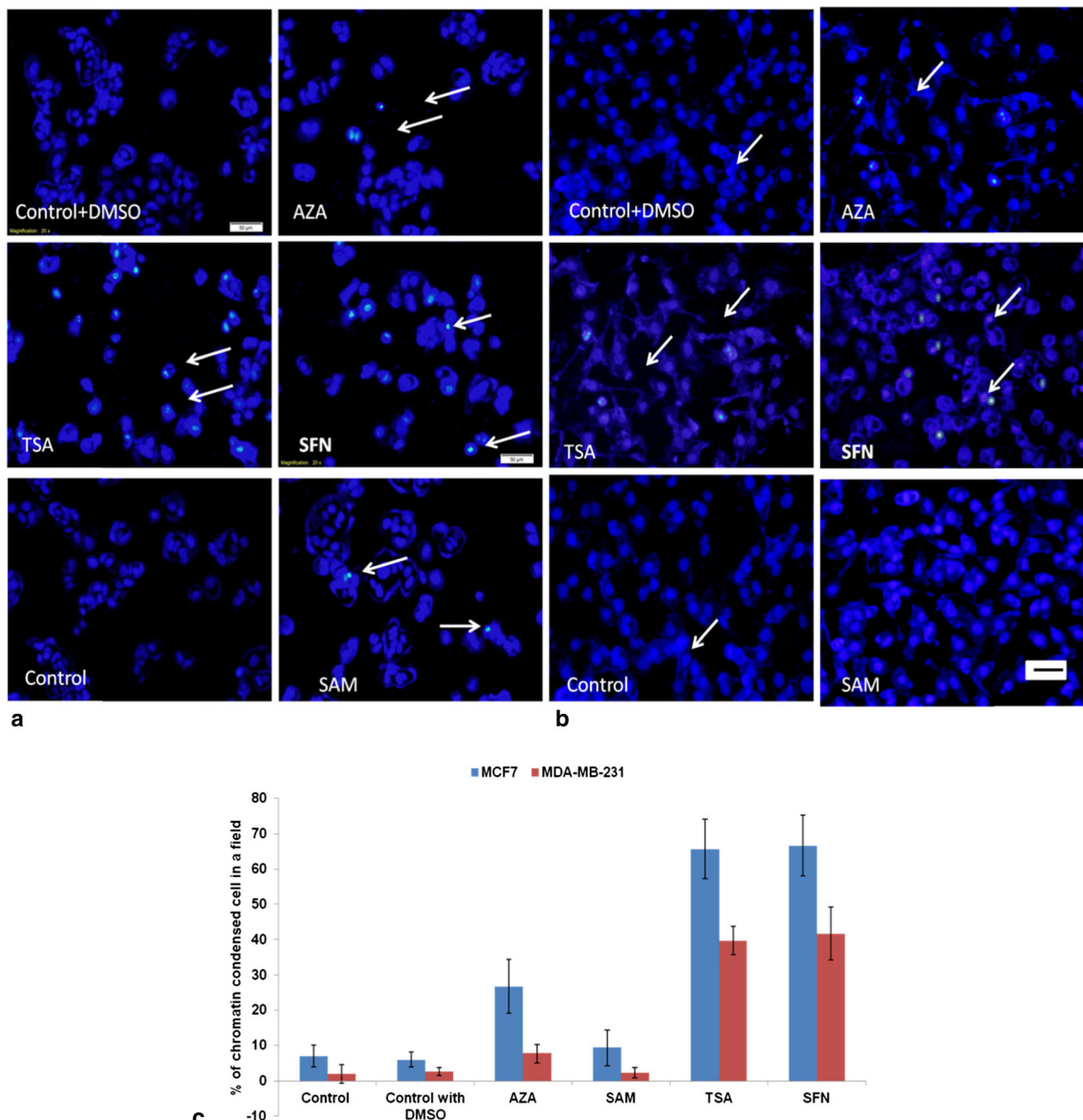


**Fig. 9** **a** MCF7 and **b** MDA-MB-231 cells were stained with Hoechst 33342 after treatment with AZA, TSA, SFN, and SAM. The representative images of Hoechst 33342 stained nuclei (arrow) are shown. **c**

Percentage of condensed nuclei of MDA-MB-231 and MCF7 are represented graphically ( $n=3$ , mean $\pm$ S.D.).  $P<0.05$ . Scale bar=20  $\mu$ m

#### TSA and SFN treatments in CAV1 knockdown MCF7 cells

CAV1 expression was significantly high in TSA- and SFN-treated cells. To confirm that CAV1 has a vital role in induce apoptosis and cell migration, we analyzed the cell migration and apoptosis induction after TSA treatment in CAV1 knockdown MCF7 cells. TSA- and SFN-treated CAV1 knockdown MCF7 cells show less apoptosis and increase cell migration than without knockdown TSA- and SFN-treated cells. Figure 9 shows that TSA- and SFN-treated MCF7 cells exhibit 65.66 and 66.78 % condensed chromatin. After CAV1 knockdown, these percentages decreased up to 36.35 and 41.84 % (Fig. 11). Migrated cell numbers

were increased after TSA and SFN treatments in CAV1 knockdown MCF7 cells that are 28.66 and 26.33, respectively (Fig. 12a(A), (B)). As compared with the previous result (Fig. 10), we observed that migration was significantly high (Fig. 12b) in CAV1 knockdown MCF7 cells.

#### Discussion

It has been previously described that CAV1 expression in cancer is stage specific. Depending on the stage of expression, CAV1 acts as a double-edged sword portraying a dual role of tumor suppressor or an oncogene [43, 44]. It is seen that the

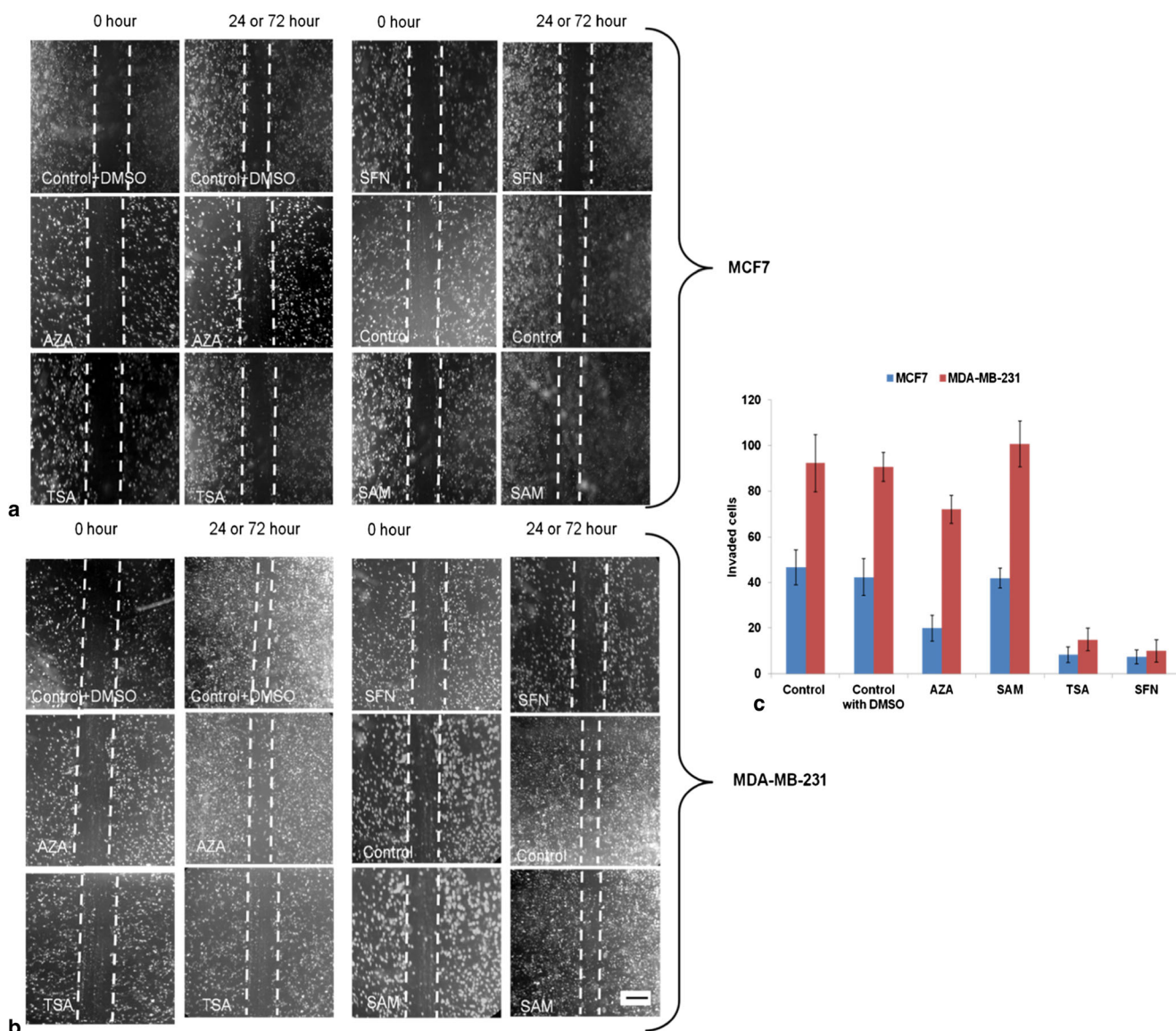


**Fig. 10** Wound healing assay. The wounded areas were analyzed under an inverted microscope **a** MCF7 and **b** MDA-MB-231 after AZA, SAM, TSA, and SFN treatments. The results were representative of three experiments each done in triplicate. Scale bar=4  $\mu$ m. **c** Quantity of migrated cells that presents an average from three experiments independently was counted. Statistical analysis ( $n=3$ , mean $\pm$ S.D.)  $P<0.05$

experiments each done in triplicate. Scale bar=4  $\mu$ m. **c** Quantity of migrated cells that presents an average from three experiments independently was counted. Statistical analysis ( $n=3$ , mean $\pm$ S.D.)  $P<0.05$

role played by CAV1 during initial stages of tumor development and during cancer progression into metastatic state is somewhat incongruous. Initially, CAV1 was reported to work as a tumor suppressor gene, but later, investigations confirmed that it also has an oncogenic property and participates in facilitating malignant transformation. CAV1 overexpression during metastasis increases cancer cell survival [45–47] and drug resistance [48, 49]; however, in primary stage, CAV1 downregulation promotes tumor growth, including breast and colon cancers [50]. In addition to promoting development and progression of colon cancer in mice, CAV1 also encourages tumor growth, possibly by altering the aerobic glycolysis in colon and breast cancers [51, 52]. This observation was well

confirmed by our initial experiments and investigation on post-operated and FPPE breast cancer tissue samples that showed that CAV1 expression in metastasis tissue samples was higher than primary breast cancer tissues (Figs. 1 and 2). However, the current study also reveals a new side regarding the function of CAV1 in breast cancer. Earlier reports have indicated that enhanced CAV1 expression during metastasis stage facilitates cancer cell mobility. However, our current study unravels for the first time that although CAV1 expression increases during metastasis stage, forced expression of CAV1 gene by epigenetic modulators can be effectively correlated with breast cancer inhibition. Our research also confirms that CAV1 is controlled by DNA methylation as well as

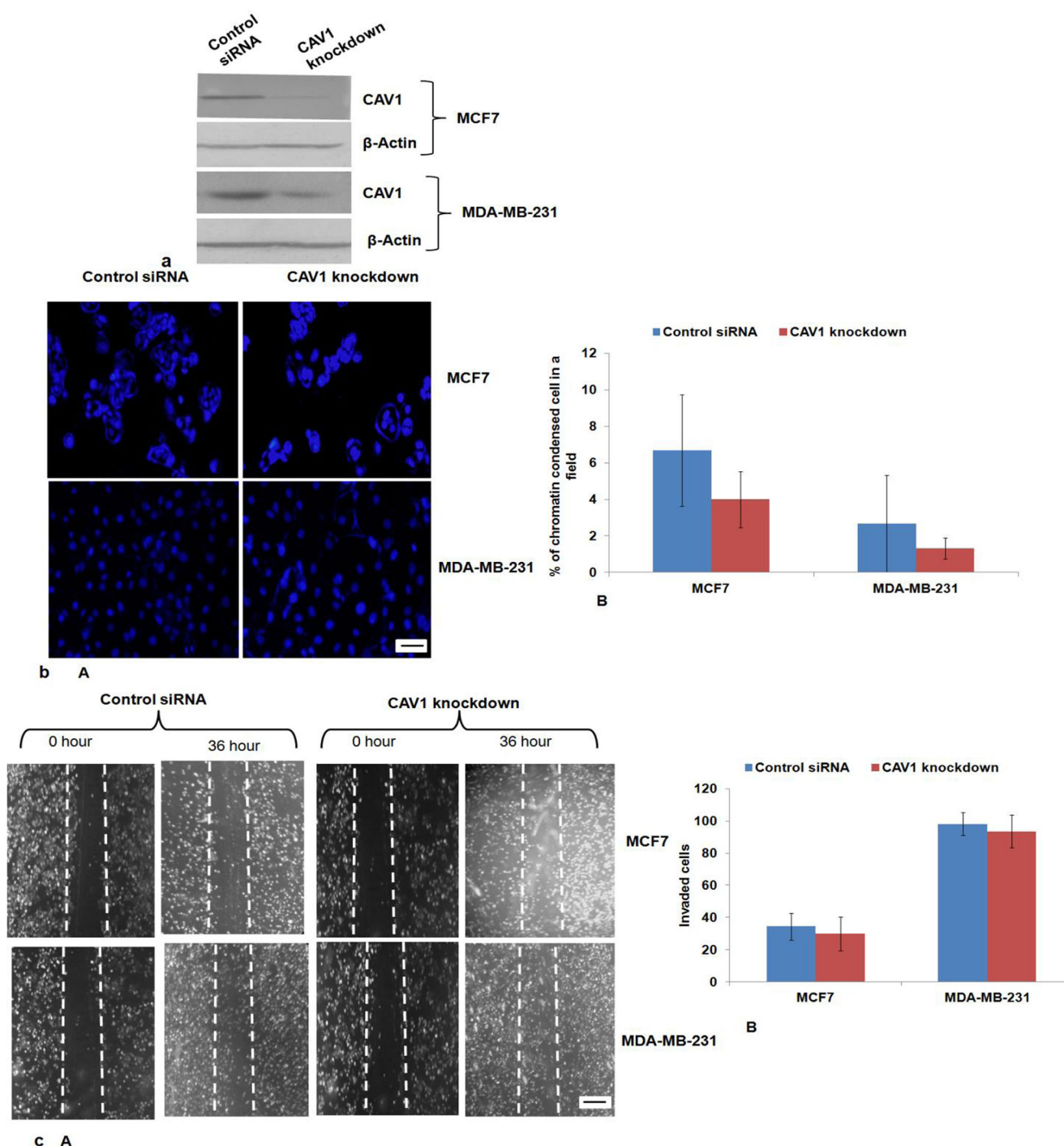


**Fig. 11** **a** CAV1 expression after CAV1 knockdown in MCF7 and MDA-MB-231. **b(A)** Cells were stained with Hoechst 33342 before and after CAV1 knockdown and **(B)** represented graphically ( $n=3$ , mean $\pm$ S.D.).  $P<0.05$ . Scale bar=20  $\mu$ m. **c(A)** After CAV1 knockdown, the wounded

areas were analyzed, and no significant changes were observed in both cell lines. Scale bar=10  $\mu$ m. **(B)** Quantity of migrated cells that presents an average from three experiments was counted ( $n=3$ , mean $\pm$ S.D.).  $P<0.05$

other epigenetic control mechanisms which are involved in CAV1 expression as seen after TSA and SFN treatments.

In an agreement with the recent understanding on the role of CAV1 in breast cancer cell lines, we have shown that the expression levels of CAV1 at transcriptome level in MDA-

MB-231 and MCF7 were differentially regulated after treatment with the epigenetic modulators like AZA, TSA, SFN, and SAM. A sharp rise in expression at mRNA level of CAV1 gene after treatment with AZA, TSA, and SFN with respect to untreated samples (Fig. 5) clearly depicts that CAV1 is directly

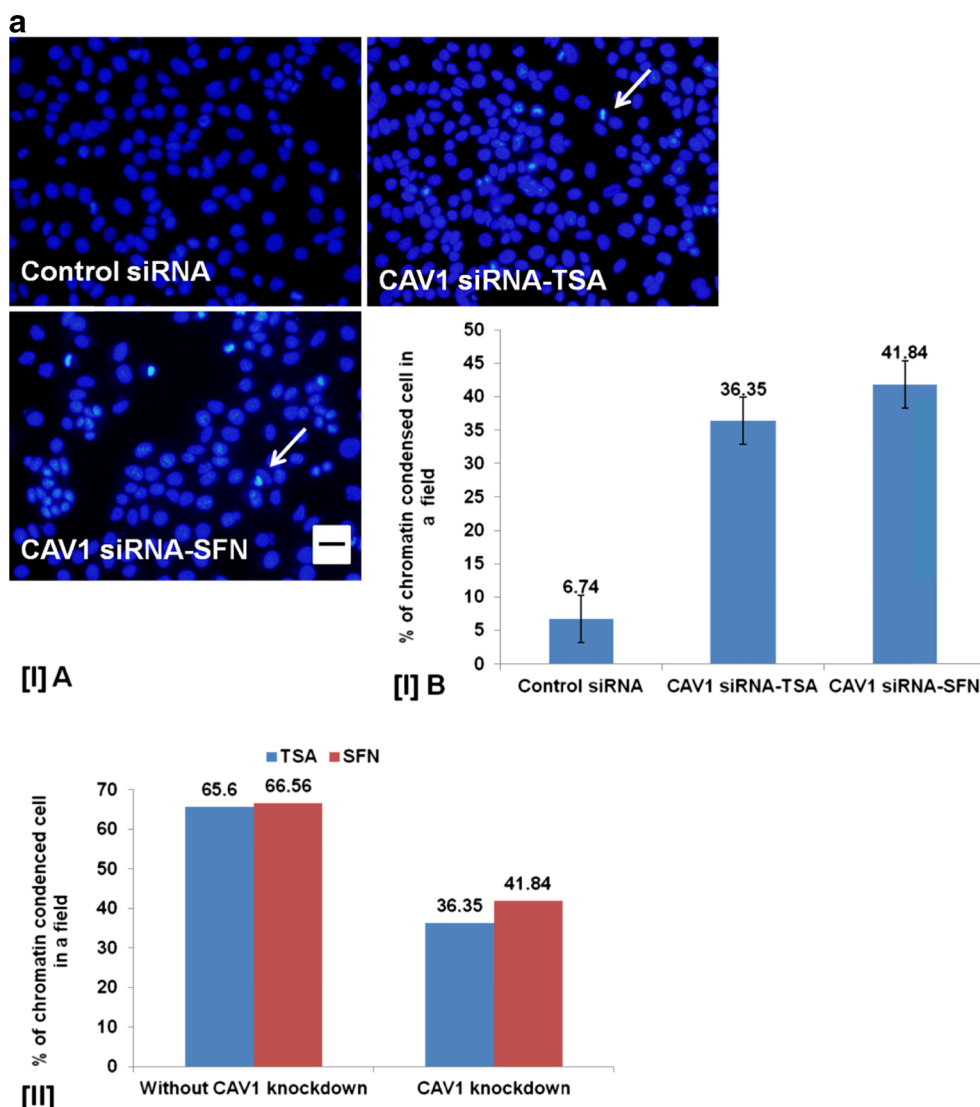


**Fig. 12** Changes in chromatin condensation and cell migration in CAV1 knockdown MCF7 cells after treatment with TSA and SFN. **a** (IA) CAV1 knockdown MCF7 cells were treated with TSA and SFN. Control siRNA-treated MCF7 cells were used as control. All treated cells were stained with Hoechst 33342 after treatment. The representative images of condensed nuclei (arrow) are shown. (IB) Percentage of condensed nuclei are represented graphically ( $n = 3$ , mean  $\pm$  S.D.).  $P < 0.05$ . Scale bar = 20  $\mu$ m. (II) Graphical representation of invaded cells in TSA treated without CAV1 knockdown and CAV1 knockdown MCF7 cells. Data of without CAV1 knockdown MCF7 was analyzed from Fig. 9. **b** (IA) CAV1

knockdown MCF7 cells were treated with TSA and SFN. Control siRNA-treated MCF7 cells were used as control. The wounded areas were analyzed under an inverted microscope. The results were representative of three experiments each done in triplicate. Scale bar = 10  $\mu$ m. (IB) Quantity of migrated cells that presents an average from three independent experiments was counted. Statistical analysis, ( $n = 3$ , mean  $\pm$  S.D.)  $P < 0.05$ . (II) Graphical representation of invaded cells in TSA treated without CAV1 knockdown and CAV1 knockdown MCF7 cells. Data of without CAV1 knockdown MCF7 was analyzed from Fig. 9

or indirectly controlled by epigenetic modifications. These findings made us wonder whether the differential mRNA expression is due to changes in methylation pattern at promoter region of CAV1 mRNA. To answer our reasoning, we analyzed DNMT expression in FFPE tissue samples and tried to connect DNMT and CAV1 expression. Moreover, we performed MSP at CAV1 promoter regions in breast cancer cell lines as well as breast cancer tissue samples. To our utter surprise, we found that unmethylated promoter is mainly

responsible for CAV1 expression in metastasis tissue samples; however, primary stage tissue samples also exhibited unmethylated promoter albeit to a much lesser level. In contrast, DNMT1 and DNMT3A are overexpressed in all types of tissue samples (Fig. 3). This indicates that although DNMT1 and DNMT3A are overexpressed in breast cancer, CAV1 gene-specific hypomethylation was also observed (Fig. 6c(A)). Therefore, a paradoxical question arises, i.e., if primary tissue samples also have unmethylated promoters,

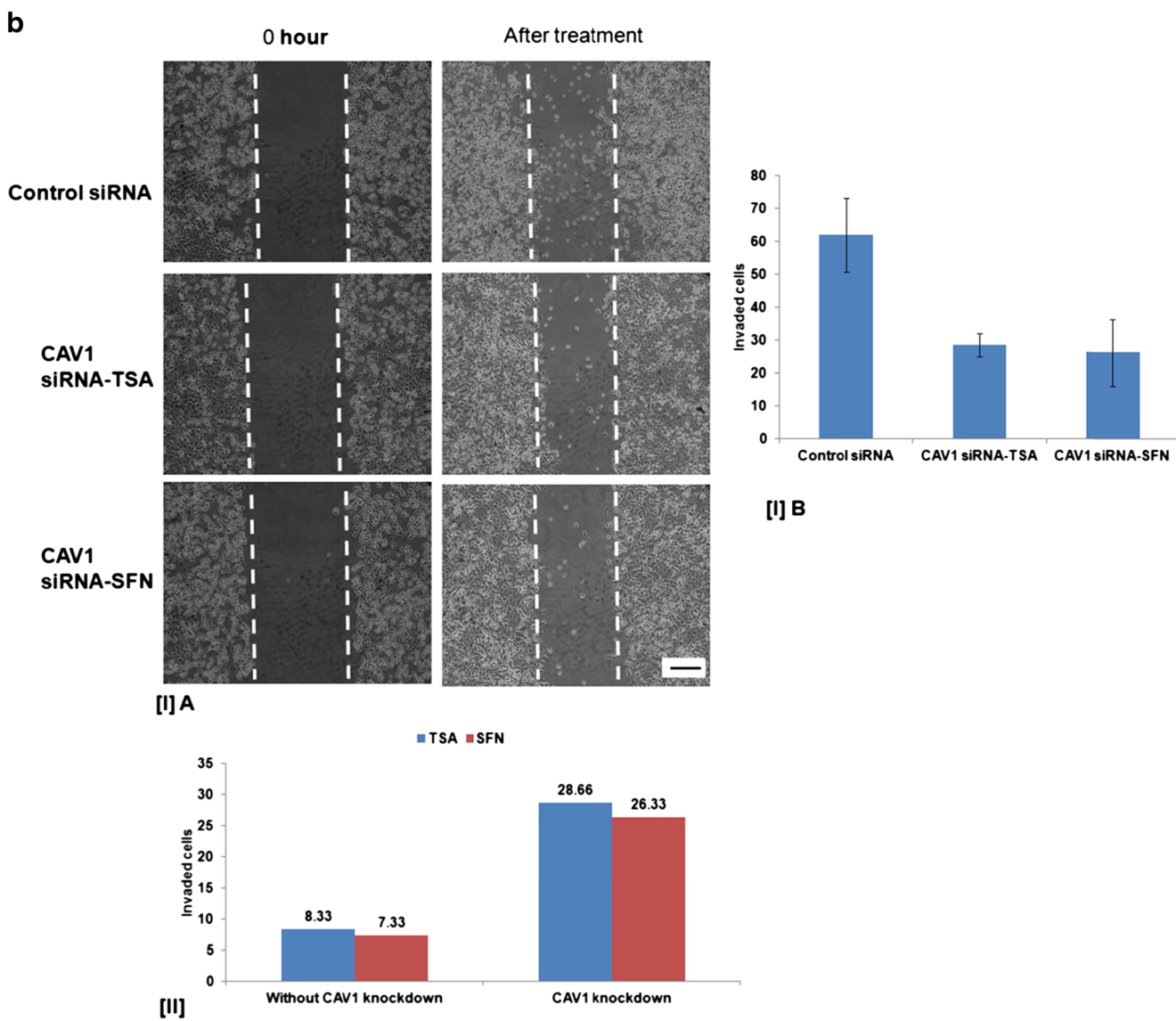


**Fig. 12** (continued)

then what is the reason behind CAV1 downregulation in primary breast cancer tissue samples? To confirm the involvement of other epigenetic mechanisms, we then proceeded with methylation analysis before and after treatments with epigenetic modulators in cancer cell lines MDA-MB-231 and MCF7. Here, we observed that only AZA-treated cells show unmethylated promoter whereas TSA- and SFN-treated cells exhibit methylated promoters. Although the promoter region is methylated, TSA and SFN are responsible for highest CAV1 expression. So, there must be another epigenetic mechanism controlling the CAV1 expression in SFN- and TSA-treated cells. TSA and SFN are potent HDAC inhibitors which lead to histone acetylation by inhibiting HDACs. CAV1 overexpression after TSA and SFN treatments indicates that increase in histone acetylation level is correlated to CAV1 overexpression. However, whether this overexpression is due to CAV1

promoter histone acetylation or due to some other factors is a matter of debate and hence requires future experimental analysis. This requires more experimental lines of evidence and also bisulfite sequencing of full CAV1 promoter as only three CpG sites were analyzed by MS PCR (Fig. 6b).

Overexpression of CAV1 mRNA level made us curious whether the change in expression at transcriptome level was substantiated by changes at protein level. To confirm the findings, we performed immunocytochemistry in order to visualize the changes in protein expression after treatment with epigenetic modulators. Immunocytochemical analysis confirms the change in expression level of CAV1 at translational level in AZA-, SAM-, TSA-, and SFN-treated cells (Fig. 7). Next, in order to quantify the fold change in expression of protein, we performed Western blotting. Data analysis further confirms that after treatment with AZA, TSA, SFN,

and SAM, there is an altered CAV1 protein expression. Western blotting experiments also indicate that in comparison to AZA and SAM, changes in expression of CAV1 were prominently more in TSA- and SFN-treated samples (Fig. 8). Next, we tried to analyze how the cellular properties were altered after treatment with epigenetic modulators. Chromatin condensation (Fig. 9) and wound healing (Fig. 10) assays also indicate remarkable decrease in migratory properties of breast cancer cell lines MDA-MB-231 and MCF7 along with induction of apoptosis. Altogether, these data clearly implicates that there exists a possible correlation between change in CAV1 expression along with altered migratory and apoptotic properties of cancer cell lines. In order to reveal the relationship between change in CAV1 expression and altered apoptosis and migratory properties in MDA-MB-231 and MCF7 cancer cell lines, we knocked down the expression of CAV1 gene in these cell lines. After knockdown of CAV1 gene, we further analyzed the apoptosis induction and migratory properties of breast cancer cell lines. CAV1-silenced MCF7 and MDA-MB-231 cell lines both behave like untreated cell lines. Although cell migration after CAV1 knockdown was same with respect to control (Fig. 11c(A), (B)), apoptosis induction is lower than control siRNA-treated cells (Fig. 11b(A), (B)). This data strengthened the possible correlation that we hypothesized regarding the role of altered CAV1 expression in induction of apoptosis and change in migratory property of breast cancer cell lines.

As per our hypothesis, CAV1 plays a key role in induction of apoptosis and inhibition of cell migration. In order to validate our findings, we knockdown the expression of CAV1 using siRNA and then observed its effect on cell migration and apoptosis induction in the presence of TSA and SFN in MCF7 cells. Since these two drugs have shown maximum upregulation of CAV1 upon treatment, so we have taken into account the effect of these drugs on cell migration and induction of apoptosis after CAV1 knockdown. Chromatin condensation analysis results depict that after CAV1 knockdown, there is a reduction in the rate of apoptosis. The rate of condensation also declines significantly in CAV1 knockdown TSA- and SFN-treated samples (Fig. 12a). As per our hypothesis, we found that after effective knockdown of CAV1 in cancer cells, there is an enhanced rate of cell migration (Fig. 11, 12). Further comparative analysis of cell migration study of drug-treated samples after CAV1 knockdown shows reduced cell migration with respect to cells not subjected to CAV1 knockdown (Fig. 12b). Cumulative data analysis of these results clearly indicated the role of CAV1 in cell migration and induction of apoptosis. These findings indicate that CAV1 acts as a potent tumor suppressor and its downregulation helps not only in cancer cell progression but also in increased survivability potentially by downregulating the apoptotic pathway. It is already reported that there are many factors like

EGFR/PI3K/AKT upregulated upon TSA treatment, which plays a crucial role in inhibiting cell migration and induction of apoptosis. Previous reports suggest that EGFR/PI3K/AKT cell survival signaling [53] and chromatin compaction-mediated changes in transcription [54] play a crucial role in TSA arbitrate cell migration inhibition and apoptosis induction. Here, in this study, we found that along with these factors, CAV1 acts in cohort in reducing cell migration and inducing apoptosis.

## References

- Patra SK. Dissecting lipid raft facilitated cell signaling pathways in cancer. *Biochim Biophys Acta*. 2008;1785:182–206.
- Patra SK, Bettuzzi S. Epigenetic DNA-methylation regulation of genes coding for lipid raft-associated components: a role for raft proteins in cell transformation and cancer progression (review). *Oncol Rep*. 2007;17:1279–90.
- Jacobson K, Mouritsen OG, Anderson RG. Lipid rafts: at a crossroad between cell biology and physics. *Nat Cell Biol*. 2007;9:7–14.
- Simons K, Toomre D. Lipid rafts and signal transduction. *Nat Rev Mol Cell Biol*. 2000;1:31–9.
- Galbiati F, Razani B, Lisanti MP. Emerging themes in lipid rafts and caveolae. *Cell*. 2001;106:403–11.
- Lin MI, Yu J, Murata T, Sessa WC. Caveolin-1-deficient mice have increased tumor microvascular permeability, angiogenesis, and growth. *Cancer Res*. 2007;67:2849–56.
- Engelman JA, Zhang X, Galbiati F, Volonte D, Sotgia F, Pestell RG, et al. Molecular genetics of the caveolin gene family: implications for human cancers, diabetes, alzheimer disease, and muscular dystrophy. *Am J Hum Genet*. 1998;63:1578–87.
- Drab M, Verkade P, Elger M, Kasper M, Lohn M, Lauterbach B, et al. Loss of caveolae, vascular dysfunction, and pulmonary defects in caveolin-1 gene-disrupted mice. *Sci (New York, NY)*. 2001;293: 2449–52.
- Razani B, Engelman JA, Wang XB, Schubert W, Zhang XL, Marks CB, et al. Caveolin-1 null mice are viable but show evidence of hyperproliferative and vascular abnormalities. *J Biol Chem*. 2001;276:38121–38.
- Gratton JP, Bernatchez P, Sessa WC. Caveolae and caveolins in the cardiovascular system. *Circ Res*. 2004;94:1408–17.
- Yu J, Bergaya S, Murata T, Alp IF, Bauer MP, Lin MI, et al. Direct evidence for the role of caveolin-1 and caveolae in mechanotransduction and remodeling of blood vessels. *J Clin Invest*. 2006;116:1284–91.
- Zhao YY, Liu Y, Stan RV, Fan L, Gu Y, Dalton N, et al. Defects in caveolin-1 cause dilated cardiomyopathy and pulmonary hypertension in knockout mice. *Proc Natl Acad Sci U S A*. 2002;99:11375–80.
- Schubert W, Sotgia F, Cohen AW, Capozza F, Bonuccelli G, Bruno C, et al. Caveolin-1(−/−)- and caveolin-2(−/−)-deficient mice both display numerous skeletal muscle abnormalities, with tubular aggregate formation. *Am J Pathol*. 2007;170:316–33.
- Ho CC, Huang PH, Huang HY, Chen YH, Yang PC, Hsu SM. Up-regulated caveolin-1 accentuates the metastasis capability of lung adenocarcinoma by inducing filopodia formation. *Am J Pathol*. 2002;161:1647–56.
- Chen ST, Lin SY, Yeh KT, Kuo SJ, Chan WL, Chu YP, et al. Mutational, epigenetic and expressional analyses of caveolin-1 gene in breast cancers. *Int J Mol Med*. 2004;14:577–82.

16. Mossman D, Kim KT, Scott RJ. Demethylation by 5-aza-2'-deoxycytidine in colorectal cancer cells targets genomic DNA whilst promoter CpG island methylation persists. *BMC Cancer*. 2010;10:366.
17. Habold C, Poehlmann A, Bajbouj K, Hartig R, Korkmaz KS, Roessner A, et al. Trichostatin a causes p53 to switch oxidative-damaged colorectal cancer cells from cell cycle arrest into apoptosis. *J Cell Mol Med*. 2008;12:607–21.
18. Parbin S, Kar S, Shilpi A, Sengupta D, Deb M, Rath SK, et al. Histone deacetylases: a saga of perturbed acetylation homeostasis in cancer. *J Histochem Cytochem*. 2013;62:11–33.
19. Meeran SM, Patel SN, Tollefsbol TO. Sulforaphane causes epigenetic repression of hTERT expression in human breast cancer cell lines. *PLoS One*. 2010;5:e11457.
20. Luo J, Li YN, Wang F, Zhang WM, Geng X. S-Adenosylmethionine inhibits the growth of cancer cells by reversing the hypomethylation status of c-myc and H-ras in human gastric cancer and colon cancer. *Int J Biol Sci*. 2010;6:784–95.
21. Schmittgen TD, Livak KJ. Analyzing real-time PCR data by the comparative CT method. *Nat Protoc*. 2008;3:1101–8.
22. Patra A, Deb M, Dahiya R, Patra SK. 5-Aza-2'-deoxycytidine stress response and apoptosis in prostate cancer. *Clin Epigenetics*. 2011;2:339–48.
23. Seervi M, Joseph J, Sobhan PK, Bhavya BC, Santhoshkumar TR. Essential requirement of cytochrome c release for caspase activation by pro-caspase-activating compound defined by cellular models. *Cell death & disease*. 2011;2:e207.
24. Braasch DA, Jensen S, Liu Y, Kaur K, Arar K, White MA, et al. RNA interference in mammalian cells by chemically-modified RNA. *Biochemistry*. 2003;42:7967–75.
25. Elbashir SM, Harborth J, Lendeckel W, Yalcin A, Weber K, Tuschl T. Duplexes of 21-nucleotide RNAs mediate RNA interference in cultured mammalian cells. *Nature*. 2001;411:494–8.
26. Sunaga N, Miyajima K, Suzuki M, Sato M, White MA, Ramirez RD, et al. Different roles for caveolin-1 in the development of non-small cell lung cancer versus small cell lung cancer. *Cancer Res*. 2004;64:4277–85.
27. Rao X, Evans J, Chae H, Pilrose J, Kim S, Yan P, et al. Cpg island shore methylation regulates caveolin-1 expression in breast cancer. *Oncogene*. 2013;32:4519–28.
28. Lin SY, Yeh KT, Chen WT, Chen HC, Chen ST, Chang JG. Promoter CpG methylation of caveolin-1 in sporadic colorectal cancer. *Anticancer Res*. 2004;24:1645–50.
29. Cui J, Rohr LR, Swanson G, Speights VO, Maxwell T, Brothman AR. Hypermethylation of the caveolin-1 gene promoter in prostate cancer. *Prostate*. 2001;46:249–56.
30. Wiechen K, Diatchenko L, Agoulnik A, Scharff KM, Schober H, Arlt K, et al. Caveolin-1 is down-regulated in human ovarian carcinoma and acts as a candidate tumor suppressor gene. *Am J Pathol*. 2001;159:1635–43.
31. Bachmann N, Haesler J, Luedke M, Kuefer R, Perner S, Assum G, et al. Expression changes of CAV1 and EZH2, located on 7q31 approximately q36, are rarely related to genomic alterations in primary prostate carcinoma. *Cancer Genet Cytogenet*. 2008;182:103–10.
32. Singh KP, Treas J, Tyagi T, Gao W. DNA demethylation by 5-aza-2'-deoxycytidine treatment abrogates 17 beta-estradiol-induced cell growth and restores expression of DNA repair genes in human breast cancer cells. *Cancer Lett*. 2012;316:62–9.
33. Mirza S, Sharma G, Pandya P, Ralhan R. Demethylating agent 5-aza-2'-deoxycytidine enhances susceptibility of breast cancer cells to anticancer agents. *Mol Cell Biochem*. 2010;342:101–9.
34. Kim SH, Kang HJ, Na H, Lee MO. Trichostatin A enhances acetylation as well as protein stability of ERalpha through induction of p300 protein. *Breast Cancer Res*. 2010;12:R22.
35. Alao JP, Stavropoulou AV, Lam EW, Coombes RC, Vigushin DM. Histone deacetylase inhibitor, Trichostatin A induces ubiquitin-independent cyclin D1 degradation in MCF-7 breast cancer cells. *Mol Cancer*. 2006;5:8.
36. Galbiati F, Volonte D, Liu J, Capozza F, Frank PG, Zhu L, et al. Caveolin-1 expression negatively regulates cell cycle progression by inducing G(0)/G(1) arrest via a p53/p21(WAF1/Cip1)-dependent mechanism. *Mol Biol Cell*. 2001;12:2229–44.
37. Neve RM, Chin K, Fridleyand J, Yeh J, Baehner FL, Fevr T, et al. A collection of breast cancer cell lines for the study of functionally distinct cancer subtypes. *Cancer Cell*. 2006;10:515–27.
38. Ostapkowicz A, Inai K, Smith L, Kreda S, Spychal J. Lipid rafts remodeling in estrogen receptor-negative breast cancer is reversed by histone deacetylase inhibitor. *Mol Cancer Ther*. 2006;5:238–45.
39. Guendel I, Carpio L, Pedati C, Schwartz A, Teal C, Kashanchi F, et al. Methylation of the tumor suppressor protein, BRCA1, influences its transcriptional cofactor function. *PLoS One*. 2010;5:e11379.
40. Du J, Zhou N, Liu H, Jiang F, Wang Y, Hu C, et al. Arsenic induces functional re-expression of estrogen receptor alpha by demethylation of DNA in estrogen receptor-negative human breast cancer. *PLoS One*. 2012;7:e35957.
41. Tone S, Sugimoto K, Tanda K, Suda T, Uehira K, Kanouchi H, et al. Three distinct stages of apoptotic nuclear condensation revealed by time-lapse imaging, biochemical and electron microscopy analysis of cell-free apoptosis. *Exp Cell Res*. 2007;313:3635–44.
42. Rodriguez LG, Wu X, Guan JL. Wound-healing assay. *Methods Mol Biol*(Clifton, NJ). 2005;294:23–9.
43. Huang C, Qiu Z, Wang L, Peng Z, Jia Z, Logsdon CD, et al. A novel FoxM1-caveolin signaling pathway promotes pancreatic cancer invasion and metastasis. *Cancer Res*. 2012;72:655–65.
44. Chanvorachote P, Chunhacha P. Caveolin-1 regulates endothelial adhesion of lung cancer cells via reactive oxygen species-dependent mechanism. *PLoS One*. 2013;8:e57466.
45. Nestl A, Von Stein OD, Zatloukal K, Thies WG, Herrlich P, Hofmann M, et al. Gene expression patterns associated with the metastatic phenotype in rodent and human tumors. *Cancer Res*. 2001;61:1569–77.
46. Arpaia E, Blaser H, Quintela-Fandino M, Duncan G, Leong HS, Ablack A, et al. The interaction between caveolin-1 and Rho-GTPases promotes metastasis by controlling the expression of alpha5-integrin and the activation of Src, Ras and Erk. *Oncogene*. 2012;31:884–96.
47. Tse EY, Ko FC, Tung EK, Chan LK, Lee TK, Ngan ES, et al. Caveolin-1 overexpression is associated with hepatocellular carcinoma tumorigenesis and metastasis. *J Pathol*. 2012;226:645–53.
48. Ravid D, Maor S, Werner H, Liscovitch M. Caveolin-1 inhibits cell detachment-induced p53 activation and anoikis by upregulation of insulin-like growth factor-I receptors and signaling. *Oncogene*. 2005;24:1338–47.
49. Belanger MM, Roussel E, Couet J. Up-regulation of caveolin expression by cytotoxic agents in drug-sensitive cancer cells. *Anticancer Drugs*. 2003;14:281–7.
50. Sagara Y, Mimori K, Yoshinaga K, Tanaka F, Nishida K, Ohno S, et al. Clinical significance of caveolin-1, caveolin-2 and HER2/neu mRNA expression in human breast cancer. *Br J Cancer*. 2004;91:959–65.
51. Ha TK, Her NG, Lee MG, Ryu BK, Lee JH, Han J, et al. Caveolin-1 increases aerobic glycolysis in colorectal cancers by stimulating HMGA1-mediated GLUT3 transcription. *Cancer Res*. 2012;72:4097–109.
52. Migneco G, Whitaker-Menezes D, Chiavarina B, Castello-Cros R, Pavlides S, Pestell RG, et al. Glycolytic cancer associated fibroblasts promote breast cancer tumor growth, without a measurable increase

- in angiogenesis: evidence for stromal-epithelial metabolic coupling. *Cell cycle (Georgetown, Tex)*. 2010;9:2412–22.
53. Zhou C, Qiu L, Sun Y, Healey S, Wanebo H, Kouttab N, et al. Inhibition of EGFR/PI3K/AKT cell survival pathway promotes TSA's effect on cell death and migration in human ovarian cancer cells. *Int J Oncol*. 2006;29:269–78.
54. Gerlitz G, Bustin M. Efficient cell migration requires global chromatin condensation. *J Cell Sci*. 2010;123:2207–17.